PHOTON AND DILEPTON PRODUCTION FROM HOT OUT-OFF-EQUILIBRIUM MEDIA *

R. BAIER, M. DIRKS

Fakultät für Physik, Universität Bielefeld
D-33501 Bielefeld, Germany

AND K. REDLICH

Institute for Theoretical Physics, University of Wroclaw
50-204 Wroclaw, Poland

(Received November 4, 1997)

The electromagnetic emissivity from QCD media away from equilibrium is studied in the framework of closed time path thermal field theory. For the dilepton rate a nonequilibrium mesonic medium is considered applying finite temperature perturbation theory for $\pi - \rho$ interactions. The dilepton rate is derived up to the order g_ρ^2. For hard photon production a quark gluon plasma is assumed and calculations are performed in leading order in the strong coupling constant. These examples are chosen in order to investigate the role of possible pinch terms in boson and in fermion propagators, respectively. The implications of the results for phenomenology are also discussed.

PACS numbers: 11.10. Wx

1. Introduction

Dilepton and photon production is one of the interesting tools to study collective effects in strongly interacting matter produced in ultrarelativistic heavy ion collisions [1, 2, 3, 4]. This is particularly evident from the recent CERN experimental data at SPS collision energy measured by the collaborations CERES/NA45 [5] and HELIOS/3 [6], which show qualitatively different behaviour of the dilepton yields in A-A as compared to p-p collisions. Extensive theoretical studies done over the last years [7, 8, 9, 10, 11, 12]

* Presented at the XXXVII Cracow School of Theoretical Physics, Zakopane, Poland, May 30–June 10, 1997.

suggest that this new behaviour of the measured dilepton yield could be related with the thermalization of the medium created in heavy ion collisions. Also the properties of the measured particle spectra at AGS and SPS energy seem to be well explained by the production from the thermal source [13].

Thermalization of a hadronic medium should be a fast process. Recent calculations in kinetic theory show that only a few elastic particle collisions are already sufficient to maintain thermal particle spectra [14]. The chemical equilibration, in contrast, could be much slower as it requires a detailed balance between different reactions with particle number changing processes. Also recent predictions of QCD inspired models like HIJING [15] or Self-Screened Parton Cascade [16] lead to similar conclusions for the partonic medium. These models indicate that the partonic medium created initially in ultrarelativistic heavy ion collisions appeared after very short time in local thermal equilibrium, however, chemical saturation is most likely never achieved before the system hadronises.

The above discussions thus show that when analysing the properties of strongly interacting matter as produced in heavy ion collisions we have necessarily to take into account nonequilibrium effects.

In this work we show how nonequilibrium effects could possibly influence the electromagnetic emissivity from QCD media. In particular we discuss soft dilepton production from $\pi - \rho$ interactions in an off-equilibrium mesonic medium and hard thermal photon production from an undersaturated quark-gluon plasma.

We apply the real time formalism of field theory with particular emphasis on the role and structure of the pinch singularities [17, 18] which appear in propagators of particles in a nonequilibrium medium.

The paper is organized as follows: in Section 2 we introduce the Keldysh representation and discuss the structure of particle propagators in nonequilibrium media. In Section 3 the dilepton rate from pi-rho scattering is derived and discussed. In Section 4 we show that there is self-consistent dynamical screening which leads to a finite photon rate in an off-equilibrium quark-gluon plasma.

2. Real time formalism and particle propagators

In order to see how nonequilibrium effects modify the structure of the particle propagators we first summarize some the important relations of the real time formulation of finite temperature field theory.

In the context of the closed time path or the Keldysh representation the bare propagator in equilibrium at finite T acquires a 2×2 matrix structure of the following general form [19, 20, 21]:

$$D^0(k) = \begin{pmatrix} \Delta_R & 0 \\ 0 & -\Delta_A \end{pmatrix} \mp 2\pi i \delta(k^2 - m^2)\varepsilon(k_0) \begin{pmatrix} n(k_0) & n(k_0) \\ \pm 1 + n(k_0) & n(k_0) \end{pmatrix}, \quad (2.1)$$

where $k = (k_0, \vec{k})$, $k^2 = k_0^2 - \vec{k}^2$; θ denotes the step function, m is the $T = 0$ mass and $n(k_0)$ is the thermal distribution function

$$n(k_0) = \frac{1}{e^{k_0/T} \mp 1}, \quad (2.2)$$

where the upper (lower) sign in the denominator of the above equation (similarly as in (2.1)) corresponds to bosonic (fermionic) fields. The $\Delta_R(\Delta_A)$ are the retarded and advanced vacuum propagators which for bosons and fermions are given by

$$\Delta^B_{R(A)}(k) = \frac{1}{k^2 - m^2 \overset{+}{(-)} i\varepsilon k_0}, \qquad \Delta^F_{R(A)}(k) = \frac{\not{k} + m}{k^2 - m^2 \overset{+}{(-)} i\varepsilon k_0}. \quad (2.3)$$

In the expressions for $\Delta_{R(A)}(k)$ the usual limit $\varepsilon \to 0$ is considered. whenever this limit is defined, *e.g.*,

$$\Delta^B_R(k) - \Delta^B_A(k) = -2\pi i \varepsilon(k_0)\delta(k^2 - m^2), \quad (2.4)$$

where $\varepsilon(k_0) = \theta(k_0) - \theta(-k_0)$ is the sign function.

To account for nonequilibrium effects we follow the approximations described in detail in [20], and more recently in [22]. It amounts only to replace the thermal $n(k_0)$, (2.2), by their nonequilibrium counterparts, *i.e.* in general by Wigner distributions $n(k_0, X)$. This corresponds in terms of the cumulant expansion to approximate nonequilibrium correlations by the second cumulant only. As a further approximation we suppress the possible dependence on the center-of-mass coordinate X, essentially assuming a homogenous and isotropic medium.

Practically as nonequilibrium distributions for bosons and fermions we take,

$$n(k_0, X) = \begin{cases} n_F(|k_0|) \\ 1 - n_F(|k_0|) \end{cases} \qquad n(k_0, X) = \begin{cases} n_B(|k_0|) \\ -(1 + n_B(|k_0|)) \end{cases} \quad \text{for} \quad \begin{matrix} k_0 > 0 \\ k_0 < 0 \end{matrix} \quad (2.5)$$

with the Jüttner parameterizations

$$n_{B(F)}(|k_0|) \equiv \frac{1}{e^{(|k_0| - \mu)/T} \mp 1} \hat{=} \frac{\lambda}{e^{|k_0|/T} \mp \lambda}, \quad (2.6)$$

or for the actual estimates just the modified equilibrium distributions

$$n_{B(F)}(|k_0|) \equiv \frac{\lambda}{e^{|k_0|/T} \mp 1}, \tag{2.7}$$

expressed by introducing the fugacity parameter [23] $\lambda \equiv e^{\mu/T}$, which is assumed to be energy independent. Obviously $\lambda \neq 1$ in case of (chemical) nonequilibrium.

We have thus seen that if the separation of the macroscopic scale X from a fast microscopic one in the sense of the Wigner transform is valid, then the relevant nonequilibrium bare propagator has formally the same structure as the corresponding one in equilibrium. This, however, is not in general true for dressed propagators where the appearance of the additional out-of-equilibrium pinch singular term is to be expected [17, 18, 24].

To show the origin and the possible appearance of pinch terms, let us consider for illustration, the selfenergy one-loop corrections to the (12) component of the scalar propagator. Denoting the selfenergy insertion by the matrix $\Pi_{ab}(p)$ we obtain the improved (12)-propagator using the Dyson equation,

$$\begin{aligned} iD^{*}_{12}(p) &\sim iD_{12}(p) + \sum_{a,b=1,2} iD_{1a}(p)(-i\Pi_{ab}(p))iD_{b2}(p) \\ &= iD_{12}(p) + i\delta D_{12}(p)\,. \end{aligned} \tag{2.8}$$

With the propagators specified in (2.1,2.3) and with the relations

$$\Pi_{11}(p) = -\Pi^{*}_{22}(p), \quad \mathrm{Im}\,\Pi_{11} = \tfrac{i}{2}(\Pi_{12} + \Pi_{21}), \tag{2.9}$$

also valid out-of-equilibrium, we obtain

$$\begin{aligned} \delta D_{12}(p) &= n(p_0, X)(\Delta^2_R(p) - \Delta^2_A(p))\mathrm{Re}\,\Pi_{11}(p) \\ &+ \tfrac{1}{2}n(p_0, X)(\Delta^2_R(p) + \Delta^2_A(p))[\Pi_{12}(p) - \Pi_{21}(p)] \\ &+ \Delta_R(p)\Delta_A(p)[n(p_0, X)\Pi_{21}(p) - (1 + n(p_0, X))\Pi_{12}(p)]. \end{aligned} \tag{2.10}$$

Here the ill-defined product $\Delta_R(p)\Delta_A(p)$ appears, giving rise to possible unpleasant pinch singularities [17, 19]. In case of equilibrium, however, it is well known that the last term in (2.10) vanishes due to the detailed balance condition,

$$\Pi_{21}(p) = e^{p_0/T}\Pi_{12}(p). \tag{2.11}$$

As a consequence (2.10) simplifies to

$$\delta D^{eq}_{12}(p) = 2\pi i\varepsilon(p_0)n(p_0)\left[\delta'(p^2)\mathrm{Re}\,\Pi(p) + \frac{1}{\pi}\boldsymbol{P}\left(\frac{1}{p^2}\right)^2 \mathrm{Im}\,\Pi(p)\right], \tag{2.12}$$

where

$$\mathrm{Re}\,\Pi(p) \equiv \mathrm{Re}\,\Pi_{11}(p), \quad \mathrm{Im}\,\Pi \equiv \tfrac{1}{2}\varepsilon(p_0)\frac{i\Pi_{12}(p)}{n(p_0)}, \tag{2.13}$$

expressed in terms of the equilibrium distribution $n(p_0)$, and in terms of the (retarded) selfenergy $\Pi(p_0 + i\varepsilon p_0, \vec{p})$ [25]. δ' denotes the derivative of the δ-function, and $\boldsymbol{P}$ the principal value.

For nonequilibrium distributions (2.5), for which obviously $(1+n)/n \neq \exp(p_0/T)$, the last term in (2.10) does not cancel and may give rise to pinch singularities, which, however, have to be regularized [18] by proper resummation.

The appearance of the pinch term in the particle propagator implies a non-trivial modification of different physical processes which are relevant in out-of-equilibrium systems. In the following we discuss how the nonequilibrium effects modify dilepton and photon rates in strongly interacting matter. In particular we show that the pinch (singular) term can be successfully regularized leading to finite rates for both dilepton and photon production from a hot mesonic and quark-gluon medium, respectively.

3. Dileptons from a nonequilibrium mesonic medium

As the first example of the application of the real time formalism to describe nonequilibrium effects we consider in this section dilepton production from a mesonic medium.

The absence of chemical equilibrium in a hadronic medium can be effectively taken into account modifying the particle distribution function [14] by the fugacity parameter λ as explained in the last section. In addition we simplify the distribution adopting the Boltzmann approximation $n(k_0, X) \simeq \lambda e^{-|k_0|/T}$, and assume that $\delta\lambda \equiv \lambda - 1$ is small $\delta\lambda \ll 1$, *i.e.* a situation not far out-off-equilibrium.

Thermal dileptons are mostly produced from hadronic decays, particle bremsstrahlung and hadron-hadron scattering. In Fig. 1 we show different particle number densities as a function of temperature for a fixed value of the baryonic chemical potential $\mu_B = 0.18$ GeV. As one can see in Fig. 1 pions and rho mesons are the most abundantly present particles in a medium in the temperature range $0.14 < T < 0.20$ GeV relevant for heavy ion collisions at SPS energy. Thus, discussing soft dilepton production in a nonequilibrium hadronic medium we consider first dileptons originating from $\pi - \rho$ scattering.

The interaction of the charged pions with the neutral massive rho meson field ρ_μ and the electromagnetic potential A_μ is described by the Lagrangian [26]

$$L = |D_\mu \Phi|^2 - \tfrac{1}{4}\rho_{\mu\nu}\rho^{\mu\nu} + \tfrac{1}{2}m_\rho^2\rho_\nu\rho^\nu - \tfrac{1}{4}F_{\mu\nu}F^{\mu\nu}, \tag{3.1}$$

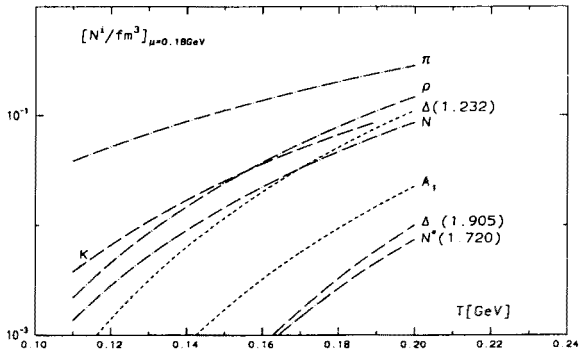

Fig. 1. Particle multiplicity per fm^3 for a baryon chemical potential $\mu_B = 0.18$ GeV as a function of temperature T.

where $D_\mu \equiv \partial_\mu - ieA_\mu - ig_\rho \rho_\mu$ is the covariant derivative, Φ is the complex pion field in the following assumed to be massless, $\rho_{\mu\nu}$ is the rho and $F_{\mu\nu}$ is the photon field strength tensor. As is well known, the $\rho\pi\pi$ coupling is rather large: $g_\rho^2/4\pi \simeq 2.9$; nevertheless we attempt an effective perturbative treatment.

The thermal emission rate of heavy photons with invariant mass M, energy E and momentum $\vec{q}$ can be obtained from the trace of the photon selfenergy tensor $\Pi^\gamma_{\mu\nu}$ as follows [2, 27]

$$\frac{dR}{dM^2 d^3q/E} = \frac{\alpha}{48\pi^4 M^2} i\Pi^\gamma_{12}(q_0, \vec{q}). \tag{3.2}$$

The virtual photon selfenergy is usually approximated by carrying out a loop expansion to some finite order. From the Lagrangian (3.1) and using the closed-time-path formalism [19, 20, 21] we calculate the dilepton rate in a thermal pionic medium at the two-loop level. Typical diagrams are shown in Figs. 2,3 and 4. The two tadpole diagrams of $O(g_\rho^2)$ are not included, since they do not contribute to the discontinuity of the photon selfenergy (3.2).

On the one loop level, Fig. 2, the photon selfenergy is expressed by the tree level particle propagators. Thus, the only difference with equilibrium calculations enters through the distribution function. In a rather straightforward way one recovers the standard expression for the Born term, $\pi^+\pi^- \to \gamma^* \to e^+e^-$, [2], which under the Boltzmann approximation and

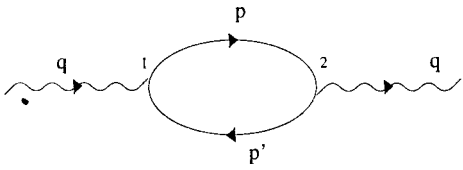

Fig. 2. One-loop diagram.

for $M < m_\rho$ reads:

$$\frac{dR}{dM^2 \frac{d^3q}{E}} \simeq (1 + 2\delta\lambda)\frac{\alpha^2}{96\pi^4}|F_\pi(M)|^2 \exp(-E/T)\,, \tag{3.3}$$

where $|F_\pi|$ is the electromagnetic pion form factor and $E^2 = \vec{q}^2 + M^2$.

The only difference of the above result with the one derived in the equilibrium medium is the appearance of the $(1+2\delta\lambda)$ factor which accounts for nonequilibrium effects. The more complete expression for the Born contribution with quantum statistics (*c.f.* (2.5)) and for arbitrary heavy photon momentum is, however, also known in the literature (see [4]).

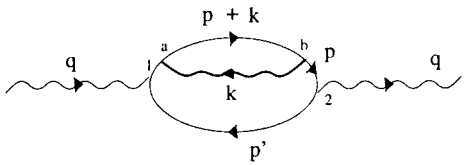

Fig. 3. Two-loop diagram: selfenergy insertion. The labels a,b =1,2 denote the type of $\pi\rho$ vertex. The solid line with momentum label k corresponds to the ρ.

For soft dileptons $M < m_\rho$ we consider in the following the mass distribution per unit space-time volume dN/dM^2d^4x[11]. To go beyond the one-loop approximation and to include the contributions due to $\pi^\pm - \rho^0$ scattering one needs to calculate the two loop diagrams shown in Figs. 3-4. There are two types of diagrams contributing to the thermal dilepton rate from $\pi - \rho$ interactions. These are the diagrams with real and virtual ρ^0 vector mesons. The processes involving real ρ^0's are due to $\pi\pi \to \rho\gamma^*$, $\pi\rho \to \pi\gamma^*$ and $\rho \to \pi\pi\gamma^*$ reactions. These contributions are obtained by cutting the two-loop diagrams (Figs. 3 and 4) such that the ρ is put on-mass shell. The virtual rho contributions, obtained by cutting the diagrams shown in Figs. 3-4 lead to $O(g_\rho^2)$ order corrections to the Born term. In the following we will discuss real and virtual rho contribution separately.

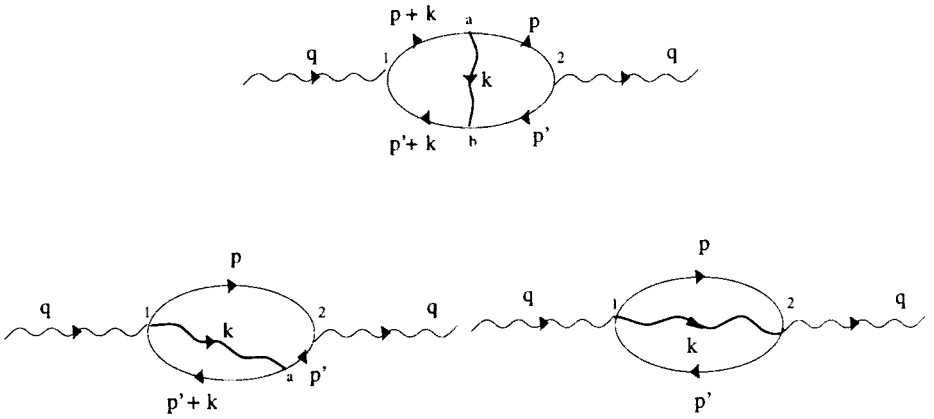

Fig. 4. Two-loop diagrams: vertex type corrections.

3.1. Dilepton rate with on-shell rho contribution

We start to discuss explicitly the contribution from the diagram shown in Fig. 3, where the selfenergy correction $\delta D_{12}(p)$ is inserted into the pionline with momentum p. The expression for $\delta D_{12}(p)$ is derived in Section 2 using the Dyson equation.

Due to the structure of the (one-loop) selfenergy correction to the pion propagator (2.10) a more careful derivation is required. Using the second and the third term of (2.10) we calculate the "real" correction to Π_{12}^{γ},

$$
\begin{aligned}
i\delta\Pi_{12}^{\gamma,\mathrm{off}}(q^0,\vec{q}) \simeq & -(-ie)^2 \int \frac{d^4p}{(2\pi)^4}\,(p+p')^2 \\
& \times\Big\{ \boldsymbol{P}\left(\frac{1}{p^2}\right)^2 n(p_0,X)\,(i\Pi_{12}(p) - i\Pi_{21}(p)) \\
& + \frac{1}{(p^2)^2 + (p_0\gamma)^2}\,(n(p_0,X) i\Pi_{21}(p) \\
& - (1+n(p_0,X)) i\Pi_{12}(p))\Big\} iD_{21}(p')\,,
\end{aligned}
\tag{3.4}
$$

where a corresponding term with $(p \leftrightarrow p')$ has to be added. The pion selfenergy $i\Pi_{12}(p)$ at one-loop order due to $\pi\rho$ interactions (3.1) is given by

$$
i\Pi_{12}(p) = g_\rho^2 \int \frac{d^4k}{(2\pi)^4}\,(2p+k)^\sigma \left(-g_{\sigma\tau} + \frac{k_\sigma k_\tau}{m_\rho^2}\right)(2p+k)^\tau\, D_{12}(p+k) D_{21}(k). \tag{3.5}
$$

In the second term in (3.4) one can recognize the contribution of the pinch term proportional to the product $\Delta_R\Delta_A$, which is not cancelled in case of

nonequilibrium distributions [17]. To regularize [18] the pinch singularity we have explicitly included a finite damping rate γ of the pion.

The pion damping rate γ is determined by the "pole" (in the lower energy half-plane) of the retarded propagator. In the following we neglect thermal corrections due to the real part of the (retarded) pion selfenergy, such that

$$\gamma \simeq -\frac{\mathrm{Im}\, \Pi(p_0, \vec{p})}{p_0}, \tag{3.6}$$

evaluated on-shell $p^2 = 0$ for positive pion energy p_0. In the one-loop approximation the dominant contribution to the absorptive part of the pion selfenergy comes from the pions thermal distribution. In the Boltzmann approximation it leads to

$$\mathrm{Im}\, \Pi(p_0 = p, p) \simeq -\frac{g_\rho^2}{4\pi}\frac{m_\rho^2}{4p}\int\limits_{\frac{m_\rho^2}{4p}}^{\infty} n(E_\pi, X) dE_\pi \simeq -\lambda \frac{g_\rho^2}{4\pi}\frac{m_\rho^2 T}{4p} e^{-\frac{m_\rho^2}{4pT}}. \tag{3.7}$$

$\mathrm{Im}\, \Pi$ vanishes for $\vec{p} = 0$, and it has its maximum near $p \simeq \frac{m_\rho^2}{4T}$. We note that (3.7) gives a positive damping rate γ, as required. In order not to overestimate the contributions arising from the $\Delta_R \Delta_A$ terms we take for the numerical estimates a momentum independent value, namely the one at the maximum,

$$p_0 \gamma \simeq -\mathrm{Im}\, \Pi\,(p_0 \simeq p, p) \simeq \lambda \frac{g_\rho^2}{4\pi}\frac{1}{e} T^2. \tag{3.8}$$

We discuss further the estimate for the dominant contribution which is due to $\pi\rho \to \pi\gamma^\star$ in the limit $\gamma \to 0$. In the Boltzmann approximation the contribution arising from (3.4) to the dilepton spectrum reads [11]

$$\frac{dN^{\mathrm{pinch}}}{dM^2 d^4x} \overset{\gamma\to 0}{\simeq} -\delta\lambda \frac{\alpha^2(g_\rho^2/4\pi)}{48\pi^4 M^2}\sqrt{\frac{\pi T^3}{2m_\rho^3}}$$
$$\times \left\{ \int\limits_{m_\rho^2}^{2m_\rho^2+M^2} du\, e^{-\frac{u+m_\rho^2}{2m_\rho T}} \int\limits_{t_{\min}}^{t_{\max}} dt + \int\limits_{2m_\rho^2+M^2}^{\infty} du\, e^{-\frac{u+m_\rho^2}{2m_\rho T}} \int\limits_{-m_\rho^2}^{t_{\max}} dt \right\} \frac{m_\rho^2 M^2}{t^2+\gamma^2}, \tag{3.9}$$

When using in (3.9) the momentum independent value for the damping γ (3.8), regularizing pinch singularities at $t^2 = 0$, the integrations can be explicitly performed. The leading term with $\gamma \to 0$ is proportional to $1/\gamma$, indicating the pinch singularity,

$$\frac{dN^{\mathrm{pinch}}}{dM^2 d^4x} \simeq -\frac{\delta\lambda}{\lambda}\frac{\alpha^2(g_\rho^2/4\pi)}{24\pi^3}\sqrt{\frac{\pi T^3}{2m_\rho^3}}\frac{m_\rho^3}{g_\rho^2/(4\pi e)T} e^{-\frac{2m_\rho^2+M^2}{2m_\rho T}}, \tag{3.10}$$

which is actually independent of the coupling g_ρ^2.

To obtain the overall rate for dilepton production with real (neutral) rho contributions one still needs to calculate the first term in (3.4). According to the calculations presented in [11], in the limit of soft dilepton mass $M < m_\rho$, this term reads

$$\frac{dN^{\text{real}}}{dM^2 d^4x} \simeq \frac{\alpha^2 g_\rho^2/4\pi}{24\pi^4 M^2}\sqrt{\frac{\pi T^3}{2m_\rho^3}}$$
$$\times\left\{\left[(1+2\delta\lambda)\int\limits_{(m_\rho+M)^2}^{\infty} ds\, e^{-\frac{s+m_\rho^2-M^2}{2m_\rho T}} + (1+\delta\lambda)\int\limits_{0}^{(m_\rho-M)^2} ds\, e^{-m_\rho/T}\right]\int\limits_{u_-}^{u_+} du\right.$$
$$\left. + (1+2\delta\lambda)2\,\boldsymbol{P}\int\limits_{m_\rho^2}^{\infty} dt\, e^{-\frac{t+m_\rho^2}{2m_\rho T}}\int\limits_{u_{\min}}^{u_{\max}} du\right\}$$
$$\times\left[2+\frac{m_\rho^2 M^2}{4}\left(\frac{1}{t^2}+\frac{1}{u^2}\right)+\frac{(m_\rho^2+M^2)^2+m_\rho^2M^2/2}{tu}-(m_\rho^2+M^2)\left(\frac{1}{t}+\frac{1}{u}\right)\right], \tag{3.11}$$

where

$$u_{\substack{+\\(-)}} = \frac{1}{2}(m_\rho^2+M^2-s)\overset{+}{(-)}\frac{1}{2}\sqrt{(s-(m_\rho+M)^2)(s-(m_\rho-M)^2)},$$
$$u_{\max} = m_\rho^2 M^2/t, \quad u_{\min} = m_\rho^2+M^2-t, \tag{3.12}$$

with $s+t+u = m_\rho^2+M^2$. The u-integration may still be performed analytically.

In the above formula we have included the corresponding contributions to the real ρ^0 processes from the two-loop vertex type diagrams of Fig. 4. The first integral in (3.12) corresponds to $\pi\pi \to \rho\gamma^*$, the second to $\rho \to \pi\pi\gamma^*$ and the third to $\pi\rho \to \pi\gamma^*$ process.

Finally the total nonequilibrium rate from real rho processes is obtained as a sum of (3.12) and the pinch term (3.10).

3.2. Higher order virtual corrections

For heavy photon production at order $O(g_\rho^2)$ we have, in order to correct the Born rate, to include virtual ρ contributions, which arise from the processes shown in Figs. 3 and 4 by cutting the diagrams in the proper way only through pion lines, without cutting the ρ line.

In some detail we describe the contribution due to the selfenergy diagram (Fig. 3). Here we take the first term in (2.10) proportional to the real part of the pion selfenergy $\Pi(p)$ and evaluate

$$i\delta\Pi_{12}^{\gamma,\mathrm{virtSE}}(q^0,\vec{q}) = (-i\epsilon)^2 \int \frac{d^4p'}{(2\pi)^3}\,(p+p')^2\,\varepsilon(p_0)\;n(p_0,X)\,\delta'(p^2)\,\mathrm{Re}\Pi(p)\,iD_{21}(p')\,. \tag{3.13}$$

The temperature-independent part of $\mathrm{Re}\Pi$ is absorbed in the definition of the $T=0$ pion mass (which we take approximately as $m_\pi = 0$). The temperature dependent part in the one-loop case under consideration is weighted by the thermal distribution either for the ρ meson or for the pion (see [28]). The first case is of $O(\exp(-m_\rho/T))$, *i.e.* negligible, the second one therefore dominates and is expected to be of $O(T^2/m_\rho^2)$, due to the presence of the $T=0$ $\rho-$ propagator in the loop (Fig. 3).

In the following we present the result for the virtual rho contribution obtained from the selfenergy diagram Fig. 3. In the limit $m_\rho \gg T$, having in mind the mass region $M \leq m_\rho$ we get for (3.13)

$$i\delta\Pi_{12}^{\gamma,\mathrm{virtSE}}(M,\vec{q}=0) \simeq -\lambda\frac{e^2}{8\pi^2}\,\frac{g_\rho^2}{4\pi}\,M^2\,\frac{T^2}{m_\rho^2}\exp(-M/T)\,. \tag{3.14}$$

In an analogous treatment the virtual $T-$ dependent contributions from the vertex type diagrams, namely from the first two of Fig. 4 have been calculated in [11]. The final results for pion annihilation including virtual rho contributions may be estimated as,

$$\frac{dN^{\mathrm{Born+virtual}}}{dM^2d^4x} \simeq \frac{dN^{\mathrm{Born}}}{dM^2d^4x}\left[\,1-\lambda\frac{7}{\pi}\,\frac{g_\rho^2}{4\pi}\left(\frac{T}{m_\rho}\right)^2\right] \tag{3.15}$$

valid for $m_\rho \gg T$, and for $M < m_\rho$. It is interesting to note that the $O(g_\rho^2)$ T-dependent corrections (3.15) are negative and could be large. It suggests to perform resummations.

3.3. Dileptons from a nonequilibrium medium — quantitative discussion

In the last sections we have shown that the real time formalism of finite temperature field theory is an adequate tool to consistently describe dilepton production from $\pi-\rho$ scattering in an off-equilibrium mesonic medium. In

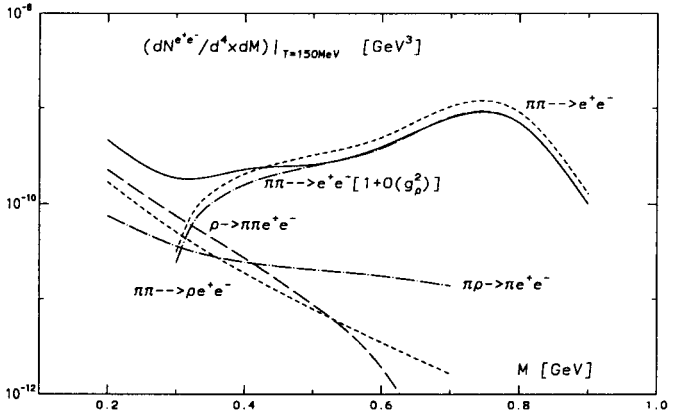

Fig. 5. Dilepton rate as a function of M at fixed T=0.15 GeV. The solid line represents the sum of all contributions.

the following we discuss quantitative properties of the dilepton rate with the emphasis on the importance of nonequilibrium effects.

In Fig. 5 we calculate the over all dilepton rate from $\pi-\rho$ scattering in an equilibrium medium that is for $\lambda = 1$. We indicate in Fig. 5 the contributions from different processes originating from the two-loop approximation of the virtual photon selfenergy. As expected the $\pi^+\pi^- \to \rho^0 e^+e^-$ reaction is a dominating source of very soft dielectrons with invariant mass $M < 0.3$ GeV. Thus, it could be a competing process with pion bremsstrahlung and Dalitz decay. At higher invariant mass $M > 0.5$ GeV the reactions with the on-shell rho meson in the initial state $\pi\rho \to \pi\ e^+e^-$ and $\rho \to \pi\pi\gamma^*$ are dominating processes calculated at the two-loop level. However, these contributions are still much smaller than the Born term due to pion annihilation $\pi^+\pi^- \to \rho \to \gamma^*$ obtained with the effective vertex from VDM. This is mostly because of the pion form factor which near the rho resonance increases the rate by more than an order of magnitude. The destructive interference of the amplitudes in the different channels and also smaller phase space are the additional reasons for this behaviour.

The contribution of the virtual rho meson calculated at $e^2 g_\rho^2$ order should be considered as finite-T corrections to the Born $\pi^+\pi^- \to \rho \to \gamma^* \to e^+e^-$ annihilation process. As seen in Fig. 5 these corrections are negative and rather large.

In order to analyse the nonequilibrium effects on dilepton production from the mesonic medium we plot in Fig. 6 the total rate characterized by

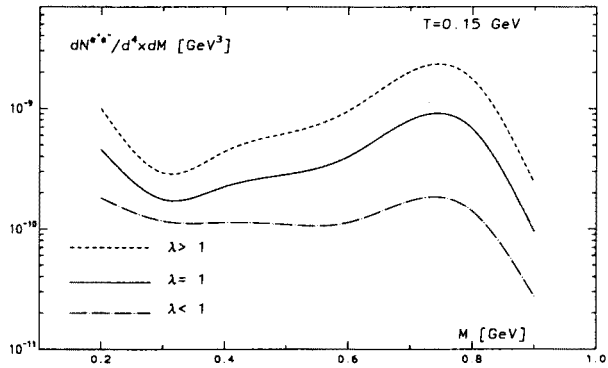

Fig. 6. Dilepton rate due to $\pi - \rho$ interactions for different values of the nonequilibrium chemical potential.

different values of the chemical potential μ. We observe that for positive μ the rate is increasing with increasing μ. However, naively one would expect an increase by a factor of λ^2, whereas the results in Fig. 6 show a much lower enhancement. Changing μ from $\mu = 0$ to $\mu = 100$ MeV only an effective increase by a factor 2 results in Fig. 6, contrary to a factor 4 expected from λ^2. This is mostly because of the negative contribution of the *pinch – singular* term summarized in (3.10). For negative values of μ, that is for $\lambda < 1$ the pinch term (3.10) is positive, thus it increases the contribution of the $\pi\rho \to \pi\gamma^*$ process in the soft part of the dilepton spectrum. Consequently for $\lambda < 1$ the spectrum is much flatter, with a less pronounced rho meson peak, as seen in Fig. 6. From this we deduce the importance of taking into account the non-trivial pinch term (3.10), which is due to the structure of the pion propagator in a nonequilibrium medium.

The possible phenomenological implications of the above results, in particular the role of $\pi - \rho$ scattering in the description of the recent CERN experimental data on soft dilepton production, have been discussed in [11, 12].

4. Hard thermal photons from nonequilibrium quark-gluon plasma

In this section we present the second example of applications of the real time formalism to describe the production of hard photons from an off-equilibrium quark-gluon plasma (QGP).

The photon yield is one of the possible observables to signal a deconfined medium produced in ultrarelativistic heavy ion collisions. To lowest order

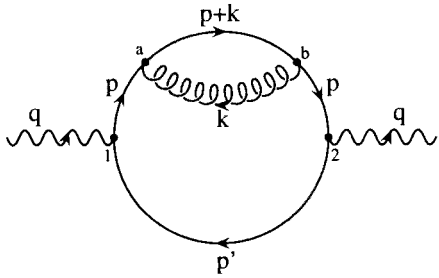

Fig. 7. The photon polarization tensor Π_{12} to first order in α_s for the real photon production. The momentum labels define the notation used in the text. External vertices are to be of type 1 and 2, respectively, internal vertices are to be summed over $a, b = 1, 2$.

in strong interactions hard photons in a QGP are predominantly produced from annihilation and Compton processes,

$$q + \bar{q} \to g + \gamma, \qquad q(\bar{q}) + g \to q(\bar{q}) + \gamma. \tag{4.1}$$

It is thus clear that the photon rate is very sensitive to the momentum distribution of quarks and gluons. Recently different QCD motivated phenomenological models [15, 16] suggest that the partonic medium created initially in heavy ion collisions reach local thermal equilibrium after very short time, however, being far away from chemical saturation. Thus, similarly as we have done for the mesonic medium (see (2.5)), we assume that parton distributions can be approximated by thermal phase space distributions, however, with nonequilibrium fugacities.

The rate of photon emission can be derived (*c.f.* 3.2)

$$E\frac{dR}{d^3q} = \frac{i}{2(2\pi)^3}\Pi_{12}{}^{\mu}_{\mu}(q), \tag{4.2}$$

from the trace of the (12)-element Π_{12} of the photon-polarization tensor calculated to leading order in the strong interaction of quarks and gluons. The relevant diagram in fixed order perturbation theory is shown in Fig. 7. The relevant (12) and (21) propagator components depend on the (off-equilibrium) distributions of quarks and gluons.

For real photons the selfenergy Π_{12} in (4.2) receives contributions only from spacelike loop-momenta $p^2 \leq 0$. The fixed order result from the diagram Fig. 7 turns out to contain IR singular contributions from small $p^2 \to 0$. For the equilibrium case it has been shown that this unphysical behavior can be cured taking hard thermal loop (HTL) contributions [29] from all orders of the quark selfenergy consistently into account [26, 30]. In the spirit of the

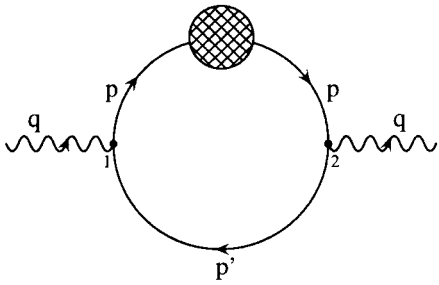

Fig. 8. The photon polarization tensor Π_{12} for soft momentum $p \sim gT$. The blob indicates the HTL-resummed quark propagator.

HTL-resummation program it is important to distinguish regions of hard from those of soft momenta [31]. We choose to separate these scales along the line $p^2 = -k_c^2$ with k_c^2 to be chosen on an intermediate scale:

$$-p^2_{\rm hard} \sim T^2 \geq k_c^2 \sim gT^2 \geq -p^2_{\rm soft} \sim g^2T^2. \tag{4.3}$$

For soft momenta resummation of leading HTL-contributions from one-loop selfenergy insertions is accomplished by substituting the effective resummed propagator as indicated by a blob in Fig. 8. In an equilibrium medium the resulting partial rate is IR finite and is shown to exactly match the hard contribution thereby introducing the thermal mass parameter m_q as an effective IR cut-off.

Turning to the off-equilibrium situation now our first task is to determine the appropriate generalization of the effective quark propagator on the hard and the soft scale.

4.1. Quark propagator — hard momentum scale

For hard momentum $-p^2 \geq k_c^2$ only the one-loop selfenergy correction to the quark propagation is to be considered. Denoting the quark selfenergy insertion by Σ the quark propagator can be obtained from the Dyson equation similar to (2.8), but in terms of the quark distribution $n_q(p_0, X)$,

$$\begin{aligned}\delta S_{12}(p) \;=\; & -n_q(p_0,X)(\Delta_R^2 - \Delta_A^2)\; \not{p} Re\Sigma(p)\; \not{p} \\ & -\tfrac{1}{2} n_q(p_0,X)(\Delta_R^2 + \Delta_A^2)\; \not{p}(\Sigma_{12} - \Sigma_{21})\; \not{p} \\ & -\Delta_R\Delta_A\; \not{p}[(1 - n_q(p_0,X))\Sigma_{12} + n_q(p_0,X)\Sigma_{21}]\; \not{p}. \end{aligned} \tag{4.4}$$

The first term in this expression corresponds to virtual corrections and vanishes for real photon production. The third genuine off-equilibrium contribution, gives rise to pinch singularity. However, due to the restricted kinematics $-p^2 \geq k_c^2$ the singularity at $p^2 = 0$ is never crossed so that in this

region the pinch combination is equivalent to the principal value appearing in the second term:

$$\frac{1}{2}\left(\Delta_R^2+\Delta_A^2\right)=\boldsymbol{P}\left(\frac{1}{p^2}\right)^2 \quad \Leftrightarrow \quad \Delta_R\Delta_A \quad \text{for} \quad -p^2\geq k_c^2>0. \tag{4.5}$$

With this relation all relevant terms in Eq. (4.4) proportional to the fermion distribution $n(p_0, X)$ are seen to cancel leaving behind the one loop corrected propagator [32]

$$\delta S_{12}(p)|_{p^2\leq -k_c^2}\triangleq -\frac{1}{(p^2)^2}\not{p}\Sigma_{12}\not{p}. \tag{4.6}$$

It has the same form as in the equilibrium case with the only difference that the quark selfenergy should be calculated with off-equilibrium distribution function.

4.2. Quark propagator — soft momentum scale

On the soft momentum scale, contrary to the discussion in the last subsection, we can not restrict the calculation of the quark propagator to the one-loop level. Here as in the equilibrium medium, one needs to carry out resummations to derive the effective propagator. In the nonequilibrium case, however, the analogous resummation program is complicated by the appearance of the extra terms as we have already seen.

The resummed propagator for the off-equilibrium situation was discussed in [17, 18] for the scalar case with the objective of providing a self consistent cut-off for the pinch contributions. Generalizing to the fermionic case resumming successive (one-loop) self-energy insertions

$$iS_{12}^{\star}(p)=iS_{12}^0+iS_{1a}^0(-i\Sigma_{ab})iS_{b2}^0+iS_{1a}^0(-i\Sigma_{ab})iS_{bd}^0(-i\Sigma_{de})iS_{e2}^0+\cdots \tag{4.7}$$

may be rearranged into the effective propagator [32, 33]

$$\begin{aligned} iS_{12}^{\star}(p)=&-n_q(p_0,X)\left(\frac{i}{\not{p}-\Sigma+i\varepsilon p_0}+\frac{-i}{\not{p}-\Sigma^{\star}-i\varepsilon p_0}\right)\\ &+\frac{i}{\not{p}-\Sigma+i\varepsilon p_0}\left[(1-n_q(p_0,X))(-i\Sigma_{12})+n_q(p_0,X)(-i\Sigma_{21})\right]\frac{-i}{\not{p}-\Sigma^{\star}-i\varepsilon p_0}, \end{aligned} \tag{4.8}$$

making use of the identities

$$\Sigma_{11}=-\Sigma_{22}^{\star}, \qquad \operatorname{Im}\Sigma=-\tfrac{i}{2}(\Sigma_{12}-\Sigma_{21}), \qquad \operatorname{Re}\Sigma=\operatorname{Re}\Sigma_{11}, \tag{4.9}$$

where $\Sigma^\star$ denotes complex conjugation and $n_{q(g)}(p_0, X)$ denotes the quark (gluon) nonequilibrium distribution functions. The effective propagator is well defined as it is regularized by the complex retarded quark selfenergy Σ.

The expression in square brackets of (4.9)

$$(1 - n_q(p_0, X))\Sigma_{12} + n_q(p_0, X)\Sigma_{21} \equiv (1 - 2n_q(p_0, X))\Sigma^- + \Sigma^+, \quad (4.10)$$

contains both leading (in the strong coupling g)

$$\Sigma^- = \tfrac{1}{2}(\Sigma_{12} - \Sigma_{21}) \sim \frac{g^2}{2\pi^2} C_F \int_0^\infty E dE (n_q(E, X) + n_g(E, X)) = m_q^2(\lambda_q, \lambda_g), \quad (4.11)$$

$$m_q^2(\lambda_q, \lambda_g) = \frac{g^2 T^2}{12} C_F \left(\lambda_g + \frac{\lambda_q}{2}\right) = O(g^2 T^2), \quad (4.12)$$

and subleading

$$\Sigma^+ = \tfrac{1}{2}(\Sigma_{12} + \Sigma_{21}) \sim p_0 g^2 \int_0^\infty dk k \left(\frac{\partial}{\partial k} n_q(k, X)\right)(1 + 2n_g(k, X)) = O(g^3 T^2) \quad (4.13)$$

contributions. In the spirit of the HTL-resummation scheme keeping only leading contributions, the resummed propagator can be rearranged into

$$iS_{12}^\star|_{HTL} = -\varepsilon(p_0) Re \left(\frac{i}{\not{p} - \Sigma_{HTL}(p) + i\varepsilon}\right), \quad (4.14)$$

where pinch-like terms have disappeared [32, 33].

The only difference of the result in (4.14) and the equilibrium resummed propagator resides in the one-loop quark selfenergy which has to be calculated with modified distribution functions (2.5).

4.3. Hard photon rate

The last step to derive the finite hard photon rate in off-equilibrium QGP is to calculate the photon selfenergy in (4.2) with the propagators derived in (4.6) and in (4.14). The calculations are well described in the literature for an equilibrium medium [30]. Here we quote only the results obtained in [32, 33].

The partial rate from the soft part

$$E_\gamma \frac{dR}{d^3q}\bigg|_{\text{soft}} = e_q^2 \frac{3\alpha}{4\pi^3} \lambda_q m_q^2(\lambda_q, \lambda_g) e^{-E_\gamma/T} \ln\left[\frac{k_c^2}{2m_q^2(\lambda_q, \lambda_g)}\right] \tag{4.15}$$

is found to be proportional to m_q^2, which also cuts the logarithm from below as expected. The parameter $k_c \sim \sqrt{g}T$ cutting the logarithm from above results from restricting the resummed calculation to soft exchanged momenta $-p^2 \leq k_c^2$.

The hard part calculated with the propagator (4.6) contains both the singular - cut-off dependent and regular contributions. The singular part of the rate in the off-equilibrium situation is obtained as [32]

$$E_\gamma \frac{dR^{\text{sing}}}{d^3q}\bigg|_{\text{hard}} = e_q^2 \frac{3\alpha}{4\pi^3} \lambda_q m_q^2(\lambda_q, \lambda_g) e^{-E_\gamma/T} \ln\left(\frac{4E_\gamma T}{k_c^2}\right), \tag{4.16}$$

the regular one as

$$E_\gamma \frac{dR^{\text{const}}}{d^3q}\bigg|_{\text{hard}} = e_q^2 \frac{2\alpha\alpha_s}{\pi^4} e^{-E_\gamma/T} T^2 \lambda_q \, C(E_\gamma, T, \lambda_q, \lambda_g), \tag{4.17}$$

with

$$\begin{aligned} C(E_\gamma, T, \lambda_q, \lambda_g) &= \lambda_q \left[-1 + (1 - \frac{\pi^2}{6})\gamma + (1 - \frac{\pi^2}{12}) \ln \frac{E_\gamma}{T} + \zeta_-\right] \\ &+ \lambda_q \lambda_g \left[\frac{1}{2} - \frac{\pi^2}{8} + (\frac{\pi^2}{4} - 2)(\gamma + \ln \frac{E_\gamma}{T}) + \frac{3}{2}\zeta'(2) + \frac{\pi^2}{12} \ln 2 + (\zeta_+ - \zeta_-)\right] \\ &+ \lambda_g \left[\frac{1}{2} + (1 - \frac{\pi^2}{3})\gamma + (1 - \frac{\pi^2}{6}) \ln \frac{E_\gamma}{T} - \zeta_+\right]. \end{aligned} \tag{4.18}$$

The appearing symbols are Euler's constant γ, the derivative of the Riemann ζ-function evaluated at $\zeta'(2)$ and the sums

$$\zeta_+ = \sum_{n=2}^{\infty} \frac{1}{n^2} \ln(n-1) \simeq 0.67, \qquad \zeta_- = \sum_{n=2}^{\infty} \frac{(-)^n}{n^2} \ln(n-1) \simeq -0.04. \tag{4.19}$$

The result Eq.(4.17) is successfully checked for consistency by noting that the constants present in the equilibrium result [30] are reproduced for $\lambda_q = \lambda_g = 1$.

Calculating the complete emission rate for real photons as the sum of the two partial rates Eqs.(4.15,4.16) and (4.17),

$$E_\gamma \frac{dR}{d^3q} = E_\gamma \frac{dR}{d^3q}\bigg|_{\text{soft}} + E_\gamma \frac{dR^{\text{sing}}}{d^3q}\bigg|_{\text{hard}} + E_\gamma \frac{dR^{\text{const}}}{d^3q}\bigg|_{\text{hard}}. \tag{4.20}$$

We see that the dependence on the arbitrarily chosen k_c cancels and the final result for the hard photon rate can be written as

$$E_\gamma \frac{dR}{d^3q} = e_q^2 \frac{\alpha\alpha_s}{2\pi^2} \lambda_q T^2 e^{-E_\gamma/T} \left[\frac{2}{3}\left(\lambda_g + \frac{\lambda_q}{2}\right) \ln\left(\frac{2E_\gamma T}{m_q^2(\lambda_q, \lambda_g)}\right) + \frac{4}{\pi^2} C(E_\gamma, T, \lambda_q, \lambda_g) \right]. \tag{4.21}$$

The above result shows that as in the equilibrium medium the generalized thermal mass is established as self consistent cut-off for the logarithmic singularity. The dynamical screening of the mass singularity seen in (4.21) here given for the distributions (2.7) actually does not depend on the explicit form of the nonequilibrium quark and gluon distribution functions. Changing the parameterization of the distribution functions enters only through the redefinition of the mass parameter in (4.14) and the constant C in (4.18), keeping at the same time the functional form of the rate unchanged.

4.4. Photon production in an expanding quark-gluon plasma

In the following we discuss the importance of nonequilibrium effects on hard photon production. Having in mind the possible phenomenological implications of the results we include the space-time evolution of the off-equilibrium quark-gluon plasma. We start with the assumption that the partonic system produced in heavy ion collisions achieves local thermal equilibrium after the time τ_i. Deviations from chemical equilibrium of quarks and gluons are measured initially by the fugacities λ_q^i and λ_g^i. Beyond this point the system expands according to the Bjorken model [34] and the chemical equilibration, that is the time dependence of fugacities is governed by rate equations.

If one assumes the off-equilibrium plasma to undergo only longitudinal expansion then according to the hydrodynamical equation the time τ-dependance of temperature is governed by the well known Bjorken's relation [34] (valid for a free gas),

$$\varepsilon \tau^{4/3} = \text{const}, \tag{4.22}$$

where for the energy density of a nonequilibrium plasma we take

$$\varepsilon = \left(\frac{8\pi^2}{15}\lambda_g + \frac{14\pi^2 n_f}{40}\lambda_q\right) T^4, \tag{4.23}$$

where $n_f \sim 2.5$ is the number of dynamical quark flavours.

For the approach to chemical equilibrium we include only the dominant reaction mechanism for parton production. These are just four processes

$$gg \leftrightarrow ggg \quad , \quad gg \leftrightarrow q\bar{q}. \tag{4.24}$$

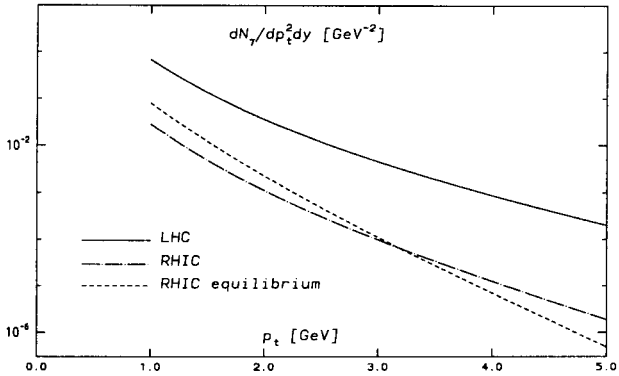

Fig. 9. Distribution of thermal photons for $y = 0$ from off-equilibrium QGP for the conditions at RHIC and LHC energies. The equilibrium result for RHIC is shown by the dotted line.

With the above processes the rate equation can be written as the following master equations in terms of the weighted reaction rates $R_{2,3}$ [35]:

$$\frac{1}{\lambda_g}\frac{d\lambda_g}{d\tau} + \frac{3}{T}\frac{dT}{d\tau} + \frac{1}{\tau} = R_3(1-\lambda_g) - 2R_2(1-\frac{\lambda_q^2}{\lambda_g^2}), \tag{4.25}$$

$$\frac{1}{\lambda_q}\frac{d\lambda_q}{d\tau} + \frac{3}{T}\frac{dT}{d\tau} + \frac{1}{\tau} = \frac{32}{9n_f}R_2(\frac{\lambda_g}{\lambda_q} - \frac{\lambda_q}{\lambda_g}),$$

describing together with (4.22) the time evolution of the parameters $T(\tau)$, $\lambda_q(\tau)$ and $\lambda_g(\tau)$.

In Fig. 9 we calculate the space-time integrated nonequilibrium photon rate (4.21). The initial conditions have been fixed for RHIC: $\tau_i \sim 0.25$ fm, $T_i \sim 0.67$ GeV, $\lambda_q^i \sim 0.064$, $\lambda_g^i \sim 0.34$ and LHC: $\tau_i \sim 0.25$ fm, $T_i \sim 1.02$ GeV, $\lambda_q^i \sim 0.082$, $\lambda_g^i \sim 0.43$ as suggested by the Self-Screened Parton Cascade model [16].

To emphasize the nonequilibrium effects we also show in Fig. 9 the photon rate for the RHIC experiment calculated with equilibrium distributions of quarks and gluons. The initial temperature $T_i \sim 0.43$ GeV is fixed requiring the initial energy density $\varepsilon_i \sim 61.4$ GeV/fm^3. The results in Fig. 9 indicate the differences between equilibrium and off-equilibrium photon yields. As expected the higher initial temperature for the chemical off-equilibrium scenario increases the yield of large $p_t > 3$ GeV photons.

Turning finally to comparisons of our results with previous studies we note first that the rate (4.21) differs in details from the results of both Refs. [36] and [37, 38]; but indeed justifies the cut-off prescription employed therein. The discrepancy with respect to [37] can be attributed to the fact that distributions for the incoming particles have been treated in Boltzmann

approximation. We find, however, that it is necessary to keep track of full quantum statistics in order for the screening to be complete.

The photon yield calculated in Fig. 9 also differs from the results given in [39]. This is related to the new structure of the off-equilibrium photon rate derived in our approach. However, although our estimate shows a different functional dependence of the photon rate on the fugacity parameters, nevertheless the numerical differences with previous estimates are small being of the order of 20%.

5. Summary

We have calculated the thermal production rate for soft dielectrons produced in off-equilibrium pionic medium including relevant reactions from $\pi - \rho$ interactions. The calculations include the $O(g_\rho^2)$ corrections arising from the two-loop contributions to the virtual photon selfenergy. We have discussed the importance of the pinch term which arises from the structure of the nonequilibrium effective particle propagator. The appearance of the pinch term modifies substantially the properties of the photon rate leading *e.g.* to the enhancement of the soft dilepton production in an undersaturated medium.

The second important result of our analysis is that we show explicitly the absence of any additional contributions from possible pinch (singular) terms to the off-equilibrium photon production rate in a quark-gluon plasma. As far as the soft momentum scale is concerned these terms are shown to be subleading with respect to the dominant hard thermal loop contributions. On the hard scale on the other hand the absence of pinch singular contributions is due to the restricted kinematics of real photon production. This result does not apply in general, *e.g.*, for virtual photon production the relevant region of phase space is sufficiently enlarged for these terms to become substantial. This has been shown to hold in our estimate of dilepton production from a mesonic medium [11] and it is also valid in the case of the quark-gluon plasma [22].

Work supported in part by the Deutsche Forschungsgemeinschaft (DFG). One of us (K. R.) acknowledges partial support by Zentrum für Interdisziplinäre Forschung (ZIF) and stimulating discussions with F. Karsch, H. Satz and D.K. Srivastava. We acknowledge discussions with D. Schiff.

REFERENCES

[1] E.L. Feinberg, *Nuovo Cimento* **34A**, 391 (1976); E. Shuryak, *Phys. Lett.* **78B**, 150 (1978).

[2] L. McLerran, T. Toimela, *Phys. Rev.* **D31**, 545 (1985).

[3] P.V. Ruuskanen, in *Quark-Gluon Plasma*, ed. R. Hwa, World Scientific, Singapore 1990); J. Alam, S. Raha, B. Sinha, *Phys. Rep.* **273**, 243 (1996).

[4] J. Cleymans, K. Redlich, H. Satz, *Z. Phys.* **C52**, 517 (1991).

[5] CERES Collab., G. Agakichiev *et al.*, *Phys. Rev. Lett.* **75**, 1272 (1995); P. Holl *et al.*, preprint CERN-SPSLC-95-35, June 1996.

[6] HELIOS/3 Collab., M. Masera, *Nucl. Phys.* **A590**, 3c (1995).

[7] D.K. Srivastava, D. Sinha, *Phys. Rev. Lett.* **73**, 2421 (1994).

[8] G.Q. Li, C.M. Ko, G.E. Brown, *Phys. Rev. Lett.* **75**, 4007 (1995); W. Cassing, W. Ehehalt, C.M. Ko, *Phys. Lett.* **B363**, 35 (1995).

[9] C. Adami, G.E. Brown, *Phys. Rep.* **224**, 1 (1993); T. Hatsuda, S. H. Lee, *Phys. Rev.* **C46**, R34 (1992); G.Q. Li, C.M. Ko, *Nucl. Phys.* **A582**, 731 (1995); F. Karsch, K. Redlich, L. Turko, *Z. Phys.* **C60**, 519 (1993); R. D. Pisarski, *Phys. Rev.* **D52**, R3773 (1995).

[10] C. Song, V. Koch, S.H. Lee, C.M. Ko, *Phys. Lett.* **B366**, 379 (1996).

[11] R. Baier, M. Dirks, K. Redlich, *Phys. Rev.* **D56**, 4344 (1997).

[12] R. Baier, M. Dirks, K. Redlich, Proceedings of the 28th International Conference on High Energy Physics, eds. Z. Ajduk and A.K. Wroblewski, World Scientific Publishing, Singapore 1997, p. 987 and references therein.

[13] J. Cleymans, H. Satz, *Z. Phys.* **C57**, 135 (1993); P. Braun-Munzinger, J. Stachel, J.P. Wessels , N. Xu, *Phys. Lett.* **B344**, 43 (1995); *Phys. Lett.* **B365**, 1 (1996); J. Letessier, A. Tounsi, U. Heinz, J. Sollfrank , J. Rafelski, *Phys. Rev.* **D51**, 3408 (1995).

[14] S. Gavin, *Nucl. Phys.* **B351**, 561 (1991); S. Gavin, P. V. Ruuskanen, *Phys. Lett.* **B262**, 326 (1991).

[15] X.-Nian Wang, M. Gyulassy, *Phys. Rev.* **D44**, 3501 (1991).

[16] K.J. Eskola, B. Müller, X.-Nian Wang, *Phys. Lett.* **B374**, 20 (1996).

[17] T. Altherr, D. Seibert, *Phys. Lett.* **B333**, 149 (1994).

[18] T. Altherr, *Phys. Lett.* **B341**, 325 (1995).

[19] N.P. Landsman, Ch.G. van Weert, *Phys. Rep.* **145**, 141 (1987).

[20] K.-C. Chou, Z.-B. Su, B.-L. Hao, L. Yu, *Phys. Rep.* **118**, 1 (1985).

[21] M.A. van Eijck, Ch.G. van Weert, *Phys. Lett.* **B278**, 305 (1992).

[22] M. Le Bellac, H. Mabilat, *Z. Phys.* **C75**, 137 (1997).

[23] S.R. de Groot, W.A. van Leeuwen, Ch.G. van Weert, *Relativistic Kinetic Theory*, North Holland, Amsterdam 1980.

[24] For a discussion of pinch singularities, which differs from [18], P.F. Bedaque, *Phys. Lett.* **B344**, 23 (1995).

[25] M. Le Bellac, *Thermal Field Theory*, Cambridge University Press, Cambridge 1996 and references therein.

[26] J.I. Kapusta, P. Lichard, D. Seibert, *Phys. Rev.* **D44**, 2774 (1991).
[27] H.A. Weldon, *Phys. Rev.* **D42**, 2384 (1990).
[28] C. Song, *Phys. Rev.* **D49**, 1556 (1994); *Phys. Rev.* **D48**, 1375 (1993).
[29] R.D. Pisarski, *Phys. Rev. Lett.* **63**, 1129 (1989); E. Braaten, R.D. Pisarski, *Nucl. Phys.* **B337**, 569 (1990); R. D. Pisarski, *Nucl. Phys.* **A525**, 175c (1991) and references therein.
[30] R. Baier, H. Nakkagawa, A. Niégawa, K. Redlich, *Z. Phys.* **C53**, 433 (1992).
[31] E. Braaten, R.D. Pisarski, T.C. Yuan, *Phys. Rev. Lett.* **64**, 2242 (1990).
[32] R. Baier, M. Dirks, K. Redlich, D. Schiff, *Phys. Rev.* **D56**, 2548 (1997).
[33] R. Baier, M. Dirks, K. Redlich, D. Schiff, *Prog. Theor. Phys.* (to appear).
[34] J.D. Bjorken, *Phys. Rev.* **D27**, 140 (1983).
[35] T.S. Biro *et al.*, *Phys. Rev.* **C48**, 1275 (1993).
[36] E. Shuryak, L. Xiong, *Phys. Rev. Lett.* **70**, 2241 (1993).
[37] M.H. Thoma, C.T. Traxler, *Phys. Rev.* **C53**, 1348 (1996). M. Strickland, *Phys. Lett.* **B331**, 245 (1994).
[38] B. Kämpfer, O. Pavlenko, *Z. Phys.* **C62**, 491 (1994).
[39] D.K. Srivastava, M.G. Mustafa, B. Müller, *Phys. Rev.* **C** (to be published).